Experimentally Measured Shear Stress in the Standpipe of a Circulating Fluidized Bed

Angela Sarra and Aubrey L. Miller
Dept. of Chemical Engineering, West Virginia University, Morgantown, WV 26505

Lawrence J. Shadle
National Energy Technology Laboratory, U.S. Department of Energy, Morgantown, WV 26507

DOI 10.1002/aic.10368
Published online March 8, 2005 in Wiley InterScience (www.interscience.wiley.com).

Shear stress measurements were obtained in the standpipe of a circulating fluidized bed (CFB) for 230-μm coke breeze particles under a variety of flow conditions. These data were combined with incremental gas-phase pressure drop readings, and an estimate of the bed weight to predict the solids-phase pressure drop. It was determined that the wall shear stress and solids-phase pressure drop are significant portions of the momentum balance and cannot be neglected when modeling frictional flow behavior of Geldart type B powders in a standpipe using the conservation of linear momentum. The combined magnitude of the axial solids-phase pressure drop and wall shear stress exceeded 48% of the total forces in the mixture momentum balance for a standpipe. However, tests indicated that the influence of the wall shear stress and axial solids pressure in the mixture momentum balance may be assumed to be negligible once minimum fluidization has been exceeded. Under packed standpipe flow conditions most literature applications treat the wall shear stress as being directly proportional to the axial solids pressure divided by a proportionality factor that does not change with solids flow rate. This assumed constant is the product of the Janssen coefficient and coefficient of friction or the stress ratio. However, shear stress measurements indicated that this proportionality factor experienced a large monotonic decrease from conditions of incipient flow, where it was at its maximum, to conditions of high volumetric fluxes, where it approached a much smaller constant value. Two packed-bed flow regimes were identified. They are the smooth flow regime, characterized as spanning from moderate to large solid volumetric flow rates, and a stick-slip regime characterized as spanning from incipient to moderate solid volumetric fluxes. © 2005 American Institute of Chemical Engineers* *AIChE J,* 51: 1131–1143, 2005
Keywords: solids-phase wall shear stress, circulating fluidized beds, standpipe, mixture momentum balance, gas solids flow

Introduction

Circulating fluid beds (CFBs) are used in a variety of chemical reactors including coal combustors and fluidized catalytic crackers (Zhang and Rudolph, 1997). These units all have standpipes that are necessary to circulate the flow of hot solids feeding the CFB riser. As in many applications that involve two-phase flow the hydrodynamics are poorly understood.

Correspondence concerning this article should be addressed to L. J. Shadle at lawrence.shadle@netl.doe.gov.

Standpipes are often operated in the frictional flow regime (defined by relative gas–solids velocities less than minimum fluidization).

In the case of coal combustion, the standpipe is critical to ensure the stable circulation of mass in the CFB. Solids recirculation stabilizes combustion while maintaining the reactor temperature in the right range for sulfur capture with limestone or dolomite. Several cases of instabilities in the circulation of mass in a CFB loop have been documented (Bi and Zhu, 1993; Shadle et al., 1999; Srivastava et al., 1998; Zhang and Fan, 1998). Other cases of instabilities have been attributed specifically to flow in a standpipe (Ginestra et al., 1980; Jones and Leung, 1985; Matsen, 1973, 1976; Rangachari and Jackson, 1982; Zhang and Rudolph, 1998).

Modeling solids movement in the frictional flow regime is necessary to understand CFB instabilities, to predict and control the circulation of mass in a CFB, and to improve scale-up capabilities of the CFB process. Several researchers suggest systems of equations for modeling frictional flow regimes in standpipes (Chen et al., 1984; Ginestra et al., 1980; Grossman, 1975; Hancher and Jury, 1959; Jones and Leung, 1985; Li, 1994; Li and Kwauk, 1989; Mohan et al., 1997; Mountziaris and Jackson, 1990; Picciotti, 1995). In addition to using equations associated with conservation of mass and momentum of the gas and solids phase (or the mixture), constitutive equations for the solids-phase shear stress and normal stress are studied (Chen et al., 1984; Grossman, 1975; Hancher and Jury, 1959; Jones and Leung, 1985; Li and Kwauk, 1989; Mohan et al., 1997; Mountziaris and Jackson, 1990; Picciotti, 1995). To better understand these constitutive equations, several researchers have attempted to estimate velocity gradients (Delaplaine, 1956; Nedderman and Laohakul, 1980; Takahashi and Yanai, 1973; Tuzun and Nedderman, 1979) and stresses (Brandt and Johnson, 1963; Delaplaine, 1956; Hancher and Jury, 1959; Li and Kwauk, 1989a,b) in the frictional flow regime.

In standpipes with solids downflow for gas–solids mixtures, there are no measurements reported for solids stresses as a function of solids flow. Solids stresses in liquid–solid-phase systems were studied as a function of bed depth and bed material, but the effect of varying the solids velocity was not presented for countercurrent flow (Brandt and Johnson, 1963; Hancher and Jury, 1959). Li and Kwauk (1989b) measured solids stresses as a function of solids velocity and bed depth. However, their system is moving-bed transport, upflow. For gas–solids downflow in a system open to the atmosphere, Delaplaine (1956) measured radial solids pressure and wall shear for several pipe diameters and bed materials. The frictional flow parameters were determined but the moving beds were not aerated as in typical closed CFB loop operations. Delaplaine (1956) asserted that the stress did not vary with solids velocity, although the effect of varying the solids velocity was not presented.

Other researchers (Matsen, 1976; Srivastava and Sundaresan, 2002; Srivastava et al., 1998) measured the bed density and gas pressure drop of gas-particle flow. The shear stress at the wall and internal stresses in the bed were inferred as the difference between the bed density and gas pressure drop. No direct measurements of these stresses were made. Such measurements resolve the sum of the solids pressure and shear stress. In a CFB standpipe, configured with a slide valve at the base of the standpipe to control solids flow, Srivastava and Sundaresan (2002) estimated a constant value for the stress ratio, μ_w/K, which was much larger than that measured in a static fluid bed during fluidization and defluidization experiments. The higher value in the CFB standpipe was consistent with our observations for the stick-slip flow regime. In their report the higher frictional factor values were attributed to electrostatic effects. In this work, the shear stress was measured as a function of solids flux for gas–solids mixtures in an aerated standpipe. Unlike the majority of the experimental studies on granular flows in which the standpipes are bottom restricted with orifice plates, the standpipe was coupled more closely to the entire CFB loop through a nonmechanical valve. Further, the solids flow rates were relatively low compared to others. In addition, continuous, real-time measurements of solids flow rates were obtained. The ability to continuously measure circulation rate and its real-time fluctuations (Ludlow et al., 2002) allowed the study of slip-stick flow.

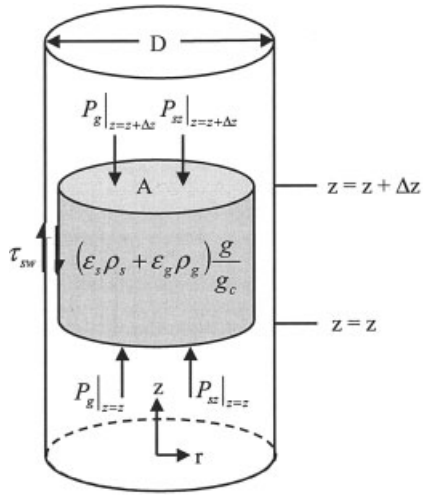

Figure 1. Standpipe force balance.

Theory

A model of the standpipe was developed from first principles, with respect to consideration of the important forces from the momentum balance. Consider the section of standpipe shown in Figure 1.

The one-dimensional (1-D) linear momentum balance on the total mixture of gas and solids is as follows:

$$\frac{\partial}{\partial t}\int\int\int_{cv}\varepsilon_s\rho_s v_{sz}dV+\frac{\partial}{\partial t}\int\int\int_{cv}\varepsilon_g\rho_g v_{gz}dV+\int\int_{cs}\varepsilon_s\rho_s\vec{v}_{sz}\cdot\vec{n}dA+\int\int_{cs}\varepsilon_g\rho_g v_{gz}\vec{v}_g\cdot\vec{n}dA=\sum F_z \quad (1)$$

The first two terms on the lefthand side are the accumulation of momentum for the gas and solids phases and, because the system is assumed to be at steady state, they are assumed to be zero. The remaining two terms on the lefthand side are the net

outflow of momentum. Assuming plug flow and constant bulk density across the control volume, the velocity into the control volume equals the velocity out, and thus the net outflow of momentum is zero.

The righthand side of Eq. 1 is the sum of the forces and its expansion yields the macroscopic form of the momentum balance

$$0 = \frac{\pi D^2}{4}(P_g + P_{sz})\big|_{z=z} - \frac{\pi D^2}{4}(P_g + P_{sz})\big|_{z=z+\Delta z} + \tau_{gw}(\pi D \Delta z) + \tau_{sw}(\pi D \Delta z) - (\varepsilon_s \rho_s + \varepsilon_g \rho_g) g \left(\frac{\pi D^2}{4} \Delta z\right) \tag{2}$$

Dividing by Δz, and taking the limit as Δz goes to zero, results in the microscopic form of the mixture momentum balance as follows

$$-\frac{\partial P_{sz}}{\partial z} - \frac{\partial P_g}{\partial z} + \frac{4\tau_{sw}}{D} + \frac{4\tau_{gw}}{D} - (\varepsilon_g \rho_g + \varepsilon_s \rho_s) g = 0 \tag{3}$$

The wall shear stress and body force terms are considered small for the gas phase and are ignored (Jones and Leung, 1985; Picciotti, 1995), resulting in the following equation in terms of significant variables

$$-\frac{\partial P_{sz}}{\partial z} - \frac{\partial P_g}{\partial z} + \frac{4\tau_{sw}}{D} - \rho_s \varepsilon_s g = 0 \tag{4}$$

Shear stress measurements were obtained experimentally using a shear vane. The gas pressure drop was experimentally measured using differential pressure transducers. The assumption that the weight deviated little from the packed state leaves the solids pressure drop as the only unknown term in the momentum balance. It was inferred by difference from the other measurements.

Existing theory (Brandt and Johnson, 1963; Delaplaine, 1956; Hancher and Jury, 1959; Jones and Leung, 1985; Mountziaris and Jackson, 1990; Picciotti, 1995) states that the wall shear stress and radial solids pressure should be related by a stress ratio, as shown in the following equation

$$\tau_{sw} = \mu_w P_{sr} \tag{5}$$

Further, the axial solids pressure and radial solids pressure are related according to the following equation

$$P_{sr} = \frac{1}{K} P_{sz} \tag{6}$$

When combined, Eqs. 5 and 6 yield the final relationship between the shear stress and axial solids pressure, expressed as

$$\tau_{sw} = \frac{\mu_w}{K} P_{sz} \tag{7}$$

Table 1. Bed Material Properties

Material	D_p (μm)	ρ_b (kg/m^3)	ρ_p (kg/m^3)	U_{mf} (m/s)
Coke breeze	230	840–880	1760	0.056

Note that $1/K$ is the Janssen coefficient, and μ_w is the coefficient of friction. The coefficient of friction is related to the angle of wall friction (δ_w) by Eq. 8 and the Janssen coefficient is related to the internal angle of friction (δ) by Eq. 9

$$\mu_w = \tan \delta_w \tag{8}$$

$$\frac{1}{K} = \frac{1 - \sin \delta}{1 + \sin \delta} \tag{9}$$

Equation 9 was obtained by Mohr stress circle analysis and is valid when the stress field is in the active state, which corresponds to the standpipe problem. A corrected form of the Janssen coefficient has also been reported in the literature as

$$\frac{1}{K} = \frac{1 - \sin \delta \cos(\beta + \delta_w)}{1 + \sin \delta \cos(\beta + \delta_w)} \quad \text{where} \quad \beta = \sin^{-1} \frac{\sin \delta_w}{\sin \delta} \tag{10}$$

This form of the equation tends to predict slightly larger values for the Janssen coefficient. Herein, the laboratory-measured values of the coefficient were based on Eq. 9. The Janssen coefficient and the coefficient of friction are properties of the bed material. Picciotti (1995) describes the stress ratio as representing the material's resistance to flow. He further states that it balances the internal property of the solids to sustain motion with the external resistance to stop motion. A higher value of stress ratio (μ_w/K) corresponds to a higher resistance to flow.

By measuring δ and δ_w using the Jenike shear cell (Jenike & Johansson Inc.) the stress ratio μ_w/K was determined for the coke breeze bed material. By substituting Eq. 7 into Eq. 4, the following expression was obtained after mathematical manipulation (Picciotti, 1995)

$$P_{sz}\big|_{z=z_1} = \frac{DK}{4\mu_w}\left[e^{-(4\mu_w/DK)(z_2 - z_1)}\right]\left(\frac{\Delta P_g}{\Delta z} + \frac{4\mu_w}{DK} P_{sz}\big|_{z=z_2} - \rho_s \varepsilon_s g\right) - \frac{DK}{4\mu_w}\left(\frac{\Delta P_g}{\Delta z} - \rho_s \varepsilon_s g\right) \tag{11}$$

Assumptions were constant solids volume fraction, constant gas pressure drop per unit length, and that the bed was in an active state of stress. Because of the assumption of constant gas pressure drop per unit length, this equation was applied over several small sections of the standpipe where measurements of the gas pressure were taken. Incremental values of the solids pressure along the standpipe were then determined. Assuming the solids pressure to be zero at the top of the bed, a solids pressure at each interval into the bed was calculated. Using measured values of the shear stress along with Eqs. 7 and 11, the stress ratio μ_w/K was obtained.

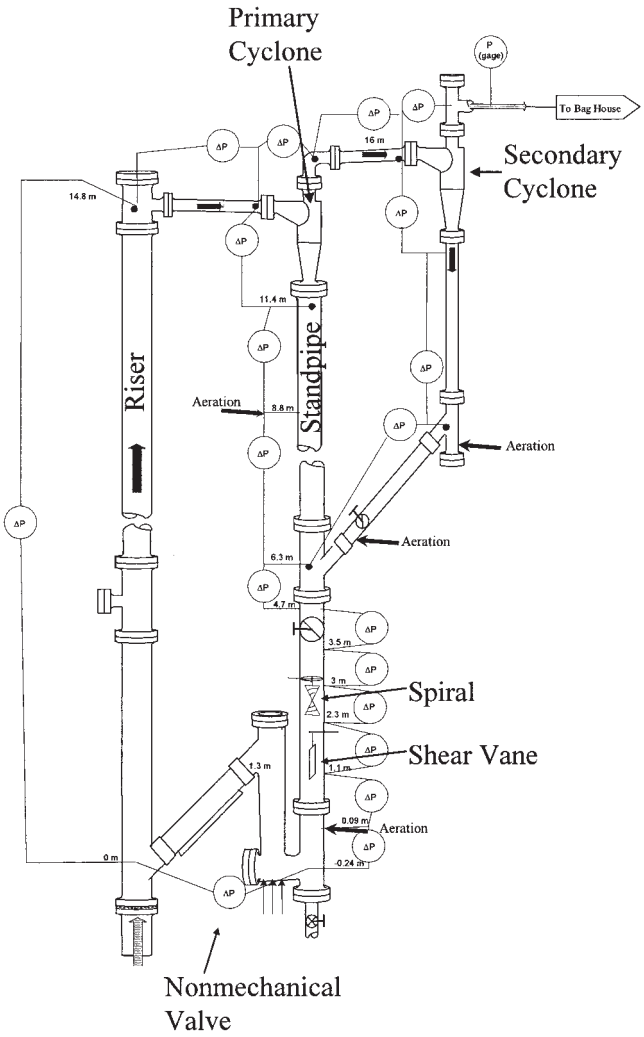

Figure 2. NETL circulating fluidized bed.

Experimental

Circulating fluidized bed

All experimental work was carried out at the National Energy Technology Laboratory (NETL). The chosen bed material was coke breeze and its properties are listed in Table 1. Particle size was characterized using the Sauter mean from sieve analysis, and the minimum fluidization velocity was measured in a 5.25-cm-diameter bubbling bed by sequentially increasing gas velocity. Particle density was measured by water displacement (Monazam et al., 2001). The material was classified as Geldart type B based on these measured properties. One advantage to using coke breeze is its high electrical conductivity that minimizes the buildup of electrostatic charge in a vessel with grounded metal components. Such electrostatic forces have been suggested to be sufficiently strong to hold solids to the vessel wall of a CFB standpipe and affect the measurement of wall shear properties (Srivastava and Sundaresan, 2002).

The CFB was configured as shown in Figure 2 (Monazam et al., 2001). This is one of the three largest cold flow public sector facilities in the United States. The riser had an inner diameter (ID) of 30.5 cm, a height of 15 m with a standpipe ID of 25.4 cm, and the system was rated at 690 kPa. Circulation rates of 54,500 kg/h for coke breeze were reached. All of the tests for this study were carried out at near atmospheric pressure and ambient temperature. The standpipe and riser were equipped with differential pressure transducers at several increments along the height. Mass flow controllers metered the aeration to the standpipe for control of the solids flow rate. Locations of mass flow controllers and pressure transducers are indicated in Figure 2. A gas pressure gradient was measured across the shear vane. The lower pressure tap was placed at 1.1 m and the upper tap at 2.3 m from the bottom of the bed.

Solids were transported from the standpipe to the riser through a nonmechanical valve. The effluent solids stream from the riser was separated from the carrier gases in primary and secondary cyclones and returned to the standpipe. This coke breeze bed material was sufficiently permeable to allow operation in the standpipe with little or no staged aeration. In other words, the gas pressure drop per unit length was relatively uniform along the entire length of the standpipe for essentially all operating conditions. CFB operations with coke breeze were never complicated by slumped sections compacting and producing zero or negative pressure gain. This supported the assumption that the solids volume fraction was relatively constant across the length of the standpipe.

The CFB was equipped with a mass flow meter (Ludlow et al., 2002) to measure the flow rate of solids in the standpipe as a function of time. This flow of solids varied with aeration rate as shown in Figure 3 for a ramp rate of 9.4 slpm (standard liters per minute). The solids circulation rate was acquired at a 0.5-Hz sampling rate. It has been shown by varying the ramp rate that for this gradual ramp the measured variables obtained from the CFB reflect a near-steady-state relationship. That is, the time-dependent effects can be neglected. There was a one-to-one correspondence between the aeration rate and the mean solids flow rate. Because all instruments were electronically connected to a data-acquisition system, abundant steady-state data were obtained by this ramping technique. Except for the solids circulation rate, all data were collected at rate of 1 Hz.

At the lower aeration rates there were instances when the solids stopped for as long as 2 s (Figure 3). This was a definitive observation of stick-slip flow. As the solids flow increased the period of flow stoppage decreased. Thus, low recorded solids flow rates were considered to experience complete solids flow stoppage for periods of <2 s. Events with solids flow readings close to zero, and appreciably lower than the mean, were also interpreted as being in the stick-slip regime.

Recent calibration of the flow meter demonstrated that the solids mass flow was linearly related to the solids velocity (Monazam et al., 2004), implying that the solids volume fraction, being the slope of the curve over the range of the measurement, was a constant. For the range of operation of the CFB covered in this article the standpipe was always packed.

Shear vane

The shear vane device was used to measure shear stress within the standpipe. It was a thin, flat metal sheet suspended from a load cell, similar in design to that used by other researchers (Delaplaine, 1956; Hancher and Jury, 1959). The

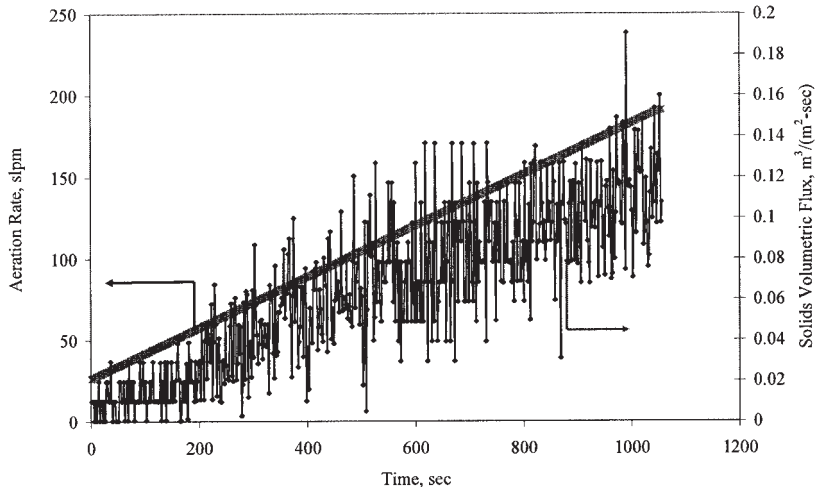

Figure 3. Solids volumetric flux (20-s running average) during an aeration ramp.

load cell measured the weight of the vane and the force exerted by the particles on the vane. The force exerted by the particles includes the shear force of the particles on the vane, and the parasitic drag on the cable and leading edge. The vane was hung along the centerline of the standpipe, where its side-to-side motion is confined by the shear of the particles. The top of the vane was located 2.4 m from the bottom of the standpipe. It was 7.62 cm in width, 61 cm in length, and 0.08 cm in thickness, as shown in Figure 4. The surface area of the vane was approximately one fifth the wall surface area of the 25.4-cm-diameter standpipe on a per unit length basis. The wall and the shear vane were made of similarly smooth materials. The wall consisted of different sections fabricated of either clear acrylic plastic or carbon steel coated with phenolic resin paint. The shear vane was fabricated of galvanized steel, polished to a smooth finish.

It was assumed that for the moving packed bed the volume fraction was constant across the standpipe radius and that consequently the shear stress measured by the vane was the same as the shear stress at the wall. Although this hypothesis is not exact, it is sufficiently close to reality to validate the findings in this research. This is consistent with an report published by Jackson (1998), in which he found that the solids pressure should be a function of the solids volume fraction. The shear stress is related to the solids pressure by the product of the friction factor and Janssen coefficient or the stress ratio (μ_w/K).

To determine the magnitude of the parasitic drag the vane length and aeration to the standpipe were varied. As the aeration was increased, the solids volumetric flux increased as shown in Figure 3. Two different aeration rates were analyzed for each of three different shear vane lengths that were otherwise identical. These six conditions are plotted in Figure 5. Regression lines are also plotted along with corresponding equations and regression coefficients (R^2), indicating good fits to the curves.

The dimensions of the leading edge and cable were unaffected by changes in the length of the vane. Thus, in Figure 5 by extrapolating the vane length to zero the contribution of the parasitic drag was determined. Therefore, at an aeration rate of 160 slpm the parasitic drag was 9.2 N and at aeration rate of 190 slpm the parasitic drag was 7.2 N. The aforementioned analysis was applied between the aeration rates of 30 to 190 slpm. The parasitic drag force and total force for each vane are plotted as a function of aeration rate, as shown in Figure 6. Unfortunately, the fact that the solids pressure steadily increased as one moved down the standpipe (see Figure 15 below) could confound this parasitic drag correction. The shear force measured by the vane was a function of the vane height; the shear stress increased with respect to distance from the top of the vane. Thus, shear stresses were indicative of a shear stress reported at a characteristic length down the vane. It will be shown that the solids pressure profiles were always linear with respect to height. Because the shear stress was directly proportional to the solids pressure (by the factor μ_w/K) the average shear stress on the vane was equal to the shear stress evaluated at the vane center. Thus, our assumption that the characteristic shear stress was at the center of each vane was appropriate for the data range studied, and the linear approximation of Figure 5 was demonstrated to be valid.

As shown in Figure 6, the force measured on all of the shear vanes decreased as the aeration increased. Also, as the vane length increased, the overall force measured increased because the area increased over which shear was measured. The parasitic drag was relatively constant over all the aeration rates. In Figure 7, the ratio of shear force to total force (including parasitic drag) is plotted as a function of the aeration rate for different vane lengths. The ratio of shear force to total force increased with increasing shear vane length. For the 0.61-m vane, the ratio was a maximum at about 40 slpm and decreased until it reached a constant value at roughly 125 slpm. Notice that the ratio was as low as 0.25 for a vane length of 0.30 m, which meant that three fourths of the total force measured was attributed to parasitic drag for this the shortest vane. The 0.61-m vane gave much better results with the ratio being roughly one half. There was an improvement in the ratio, in going from a 0.61 m to 1.06 m in length, but this improvement was small. It was desirable to take the measurement over the smaller length of 0.61 m to decrease the size of the control volume, and maintain the assumption that the shear changed little along the length of the control volume. For this reason the 0.61-m vane length was selected for the shear measurements.

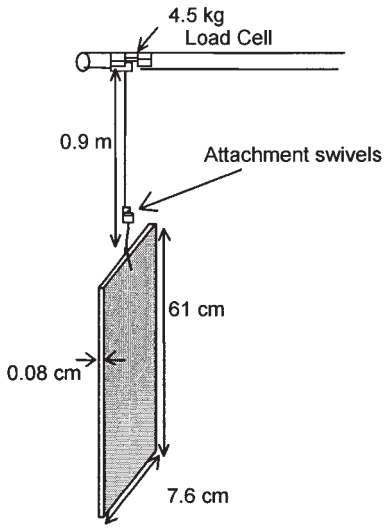

Figure 4. Shear vane.

The ratio of shear force to total force was fitted with a polynomial that was used as a correction factor to remove the parasitic drag from the raw shear vane measurements.

Results and Discussion

Shear stress in a stationary bed

Shear stress measurements were obtained in a stationary bed that was 25.4 cm × 2.44 m (diameter × height). In fact, the standpipe equipment was used as the bed. This was affected by terminating the flow of aeration to the standpipe's nonmechanical valve and also reducing the flow of air to the riser, therefore eliminating the flow of solids through the standpipe. The response of the static bed was measured in the standpipe using an increasing aeration ramp, with the data range varying from packed to fluidized. The results are plotted as a function of aeration rate instead of superficial gas velocity because the split of air going up or down the bed could not be determined. For this bed the solids volume fraction was assumed to be constant at the bed density at minimum fluidization of 840 kg/m^3. Because the solids pressure was calculated as the residual of the force balance of Eq. 4 and the vibrated bed density is 880 kg/m^3, the solids pressure drop ($-\Delta P_s/L$) may have an error up to 0.39 kN/m^3 by making this assumption. The gas pressure drop ($\Delta P_g/L$), shear stress ($-2\tau_{sw}/R$), solids pressure drop ($\Delta P_s/L$), and weight of the bed were plotted as a function of aeration rate in Figure 8 using the shear vane to determine the wall shear stress. The shear stress on the vane was calculated as the total force minus the parasitic drag divided by the total cumulative area of both sides of the vane. For the purpose of direct comparison the forces were all normalized by direct manipulation of the momentum balance. In the case of the shear stress the term was divided by $-R/2$ and the other forces by L.

Momentum balance components were measured as the aeration rate was ramped down from a value slightly above minimum fluidization. Increasing ramp rate measurements were also made, but the incipient flow caused hysteresis and large decreases in the shear stress were observed at random and irreproducible aeration rates. For the down ramps, the gas pressure drop ($-\Delta P_g/L$) remained constant until the aeration rate dropped below 150 slpm, then it decreased monotonically with decreasing aeration rate, which is typical for a fluidization curve. This rate corresponded to a superficial gas velocity of 0.049 m/s, which is comparable to the experimentally measured minimum fluidization velocity of 0.056 m/s. Note that as a consequence of the backpressure created by the bubbling bed in the riser, the gas pressure drop ($-\Delta P_g/L$) at zero aeration was a nonzero value. The shear stress ($-2\tau_{sw}/R$) continuously decreased as the aeration rate increased, until it was nearly zero at minimum fluidization. Slightly negative measurements were obtained at the higher aeration rates. The shear vane may become nearly buoyant under these conditions. The solids-phase pressure drop ($-\Delta P_s/L$) continuously decreased as the aeration rate increased. At the higher aeration rate of 190 slpm, the solids-phase pressure drop in the bed was close to zero at a value of 0.75 kN/m^3. Also the gas-phase pressure drop ($-\Delta P_g/L$) approached the density of coke breeze at minimum fluidization, 840 kg/m^3. These measurements indicated that the assumption of the weight of the bed being equal to the pressure drop was valid at and above minimum fluidization. From these data it was clear that the shear stress and solids pressure gradient must be included in the linear momentum balance when modeling standpipes that are to be operated below minimum fluidization.

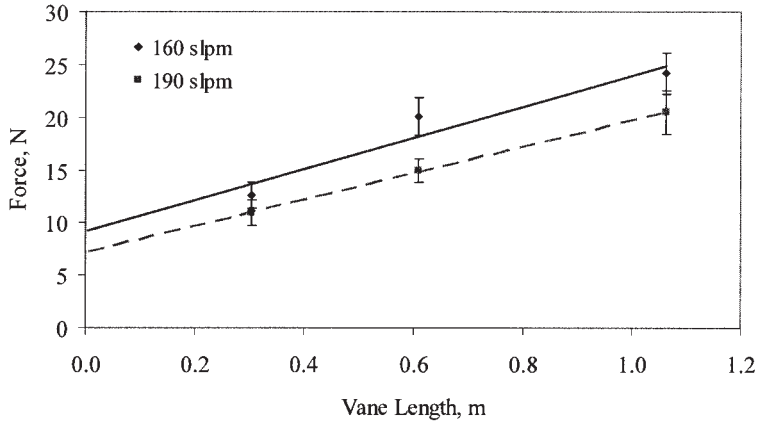

Figure 5. Steady-state (5-min averages) analysis of the parasitic drag.

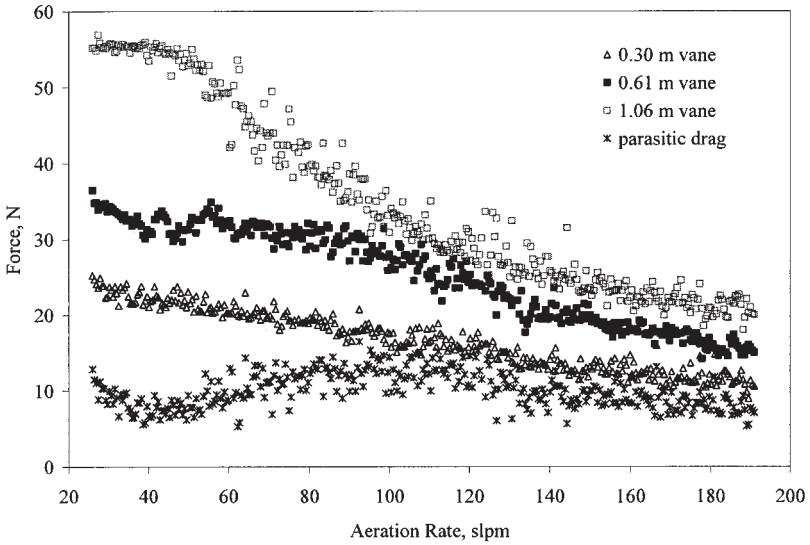

Figure 6. Total force measured for each vane length and parasitic drag.

Shear stress in a circulating standpipe

The gas pressure drop, shear stress, solids pressure drop, and weight of the bed are plotted as a function of solids volumetric flux in Figure 9. These data were obtained using a slow ramp of the aeration rate. All measured variables appeared to be approaching a limiting value as the volumetric flux increased. This was most obvious in the case of the shear stress. During the ramp the gas-phase pressure drop ($-\Delta P_g/L$) increased linearly with volumetric flux from 0.3 to 3.7 kN/m^3, which in terms of magnitude corresponded to 2 to 22% of the total forces. The magnitude of the wall shear stress decreased from 27 to 6% of the total forces as volumetric flux increased. It approached a limiting value of 1 kN/m^3 as the volumetric flux continued to increase. The solids-phase pressure drop ($-\Delta P_s/L$) varied by 2 kN/m^3 and reached a plateau at volumetric fluxes between 0.03 and 0.06 m^3 m^{-2} s^{-1}, which spanned the point where the gas-phase pressure drop ($-\Delta P_g/L$) and shear stress were equal.

Because direct measurements of the solids-phase density were not available, it was assumed that bed density was constant midway between vibrated packed and minimally fluidized at 860 kg/m^3. Standpipe bed level measurements were consistent with little or no change in bed density. That is, calibration of the solids flow in the standpipe indicated a nearly linear relationship between the solids mass flow and velocity (Monazam et al., 2003). In addition, calculation on the effect of varying the bed voidage (between packed and fluidized) had no discernible impact on the distribution of forces found in Figure 9. The uncertainty produced by this assumption produced a maximum error of 0.20 kN/m^3 with respect to both the solids-phase density and the solids-phase pressure drop per unit length, as inferred from the other measurements.

The variance in the gas-phase pressure drop ($-\Delta P_g/L$) was small at low values of the solids volumetric flux (Figure 9). Large fluctuations in the wall shear stress ($-2\tau_{sw}/R$) were observed for similarly large values of the volumetric flux. At a

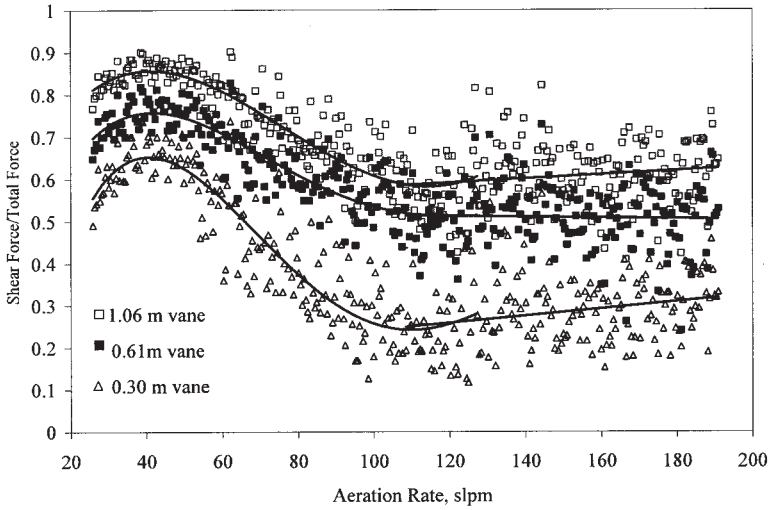

Figure 7. Ratio of shear force/total force (parasitic drag study).

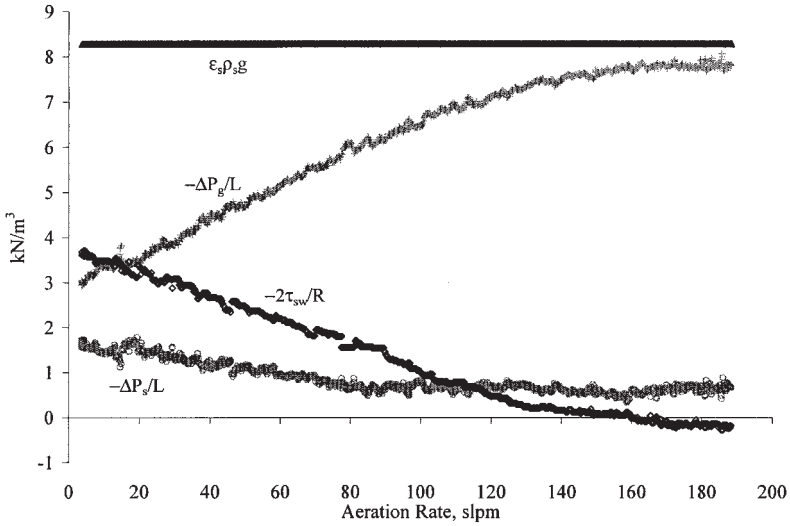

Figure 8. Momentum balance components for a stationary bed.

solids volumetric flux of about 0.05 $m^3\ m^{-2}\ s^{-1}$, a shift occurred in these directly measured variables. The variance in the shear stress became measurably smaller and that of the gas-phase pressure drop measurably larger. These changes occurred simultaneously with two measured variables and appeared to mark a transition point with respect to the operation of the bed. From visual observation, the bed operated in a stick-slip mode (solids volumetric flux switched continuously between stagnant and flowing states) at low solids flow rates. At the transition point the flow continued to fluctuate but became smoother and the sticking stopped (Figure 3). The bed operational data were examined to determine whether there were any changes in physical properties of the bed that would explain or mark the occurrence of the transition. Later in this paper (Figure 13 below) it will be shown that onset of the transition appeared to follow changes in the value of the stress ratio (μ_w/K).

It was determined that the transition was not accompanied by a change in the flow direction of the gas in the standpipe and the standpipe was always operated in a packed state. Assuming no variation in the gas velocity with respect to radial distance, Leung and Jones (1985) describe the slip velocity in a standpipe as

$$v_{sl} = \frac{U_g}{\varepsilon} - \frac{U_s}{1-\varepsilon} \tag{12}$$

where $v_{sl} > U_{mf}/\varepsilon_{mf}$ for fluidization to occur.

For coke breeze the minimum superficial fluidization velocity divided by the void fraction at minimum fluidization was 0.108 m/s, as determined from packed bed experiments. From the gas-phase momentum balance (assuming constant volume fraction), the packed bed data of Figure 8 were directly fitted to an equation using the velocity dependency from the Ergun equation, where the gas-phase pressure drop was equated with the drag as follows

$$-\Delta P_g/L = C_1 v_{sl} + C_{sl} v_{sl}^2 \tag{13}$$

It was determined that, over the entire range of operation shown in Figure 9, the time-averaged gas flow always traveled

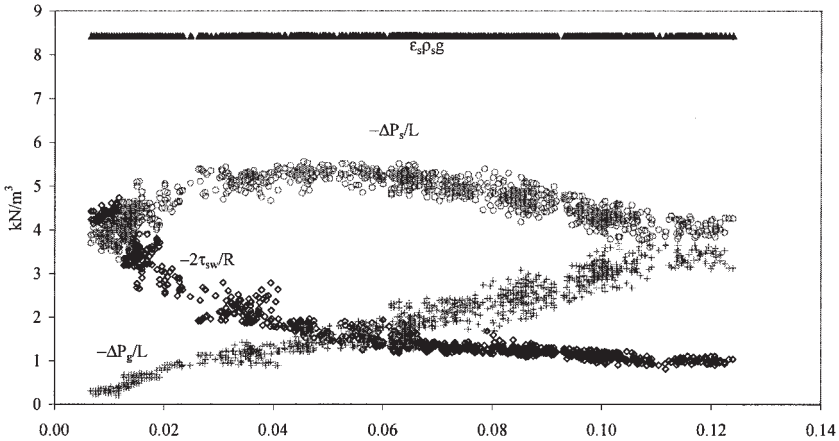

Figure 9. Momentum balance components vs. solids volumetric flux for continuously ramped aeration.

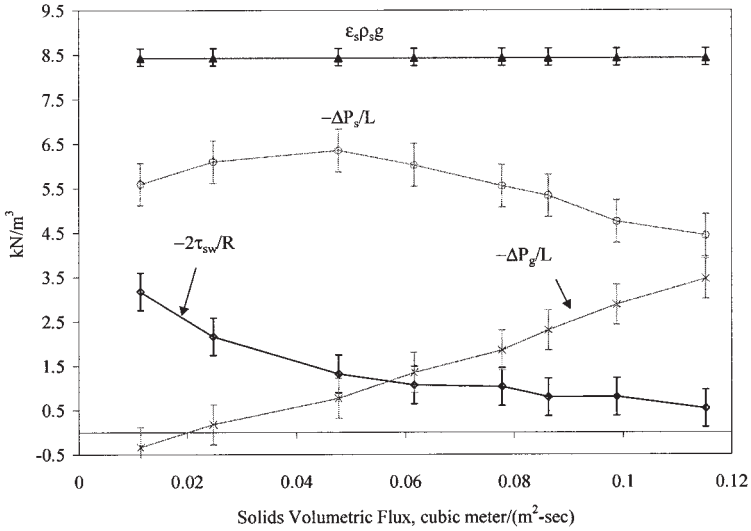

Figure 10. Momentum balance components vs. solids volumetric flux for steady-state measurements (5-min averages).

downward in the standpipe and that the flow of gas increased with increasing solids velocity (solids volumetric flux). Of course, when one considers the instantaneous solids flow stoppage in stick-slip flow we must acknowledge that the gas may experience brief transient flows in an upward direction. However, the criterion for minimum fluidization was never close to being obtained. Only at the highest solids flux rates did the velocity of the solids relative to the wall achieve flows in excess of the minimum fluidization velocity.

In Figure 10 the momentum balance measurements were evaluated under steady-state conditions by sequentially increasing the standpipe aeration in fixed increments instead of continuously ramping the aeration with time. The trends for shear stress, gas pressure drop ($-\Delta P_g/L$), solids pressure drop ($-\Delta P_s/L$), and bed weight were similar to the aeration ramp of Figure 9. Slightly higher values for the shear stress were seen in the ramps because of the larger dynamic inventory associated with ramp conditions. The general magnitude of the forces was the same. It does not appear that the ramping procedure resulted in any significant differences between the ramped and steady-state measurements. The error bars on Figure 10 were based on $\pm$2SDs for the statistical tests, assuming the error was uniformly distributed across the operating range. Because the bulk density was taken to be the mean of the vibrated density and density at minimum fluidization, the error in bulk density ranged between these two values.

Average values of the solids volumetric flux along with the corresponding values at 2SDs are tabulated in Table 2. These uncertainties reflected the large variation typical of real-time measurements of solids velocity in a CFB (Ludlow et al., 2002). The variability in solids flux seemed to increase with increasing flux. At lower fluxes, the instantaneous flux occasionally dropped to zero, producing a skewed distribution of velocities indicative of slip-stick flow (Figure 3). For example, at a flux of 0.025 $m^3\ m^{-2}\ s^{-1}$ there was a significant probability that the flux would reach zero based on the fact that twice the standard deviation was greater than the average value. At higher fluxes the fluctuations were not bounded in this manner (that is, did not drop to zero) and sticking was unlikely. At higher volumetric flow rates the deviation/mean was smaller, resulting in a smoother solids flow.

A fully randomized and duplicated 2×2 factorial design experiment was run to quantify the measured uncertainty for the effect of solids volumetric flux and total gas pressure drop in the standpipe on the solids wall shear stress. The raw data are given in Table 3. The solids volumetric flux was controlled at two levels, 0.035 and 0.07 $m^3\ m^{-2}\ s^{-1}$, and the total gas pressure drop in the standpipe was independently controlled at two levels, 22 and 25 kPa. An unbiased estimate in the amount of variability for each of these parameters was obtained from these statistical experiments. This experiment was a good example of the repeatability of shear stress measurements and gas pressure drop measurements. The analysis of variance is presented elsewhere (Sarra, 2001). At the higher solids flow rates through the standpipe there was no measurable statistically significant effect of either solids flow or gas pressure drop on the shear stress. This can be considered a characteristic feature of standpipe flow in a smooth packed-bed flow regime. Thus, when operating at solids flow rates above the stick-slip flow regime the measured shear was found to be unaffected by either the solids flow or the gas pressure drop (Figures 9 and 10). The shear stress component ($-2\tau_{sw}/R$) did not vary statistically for solids fluxes $> 0.06\ m^3\ m^{-2}\ s^{-1}$, and the decrease in stress between the fluxes of 0.01 and 0.06 $m^3\ m^{-2}\ s^{-1}$ was real. The gas pressure drop per unit length increased monotonically with increasing solids flux. We suspect that the changes in the shear stress at the lower solids fluxes (slip-stick flow) are a result of

Table 2. Standard Deviation of Sequential Solids Flux Data

$\overline{\nu_{sz}}$ ($m^3\ m^{-2}\ s^{-1}$)	$(\sigma\nu_{sz})/\overline{\nu_{sz}}$	$2 \times (\sigma\nu_{sz})$ ($m^3\ m^{-2}\ s^{-1}$)
0.011	0.73	0.016
0.025	0.64	0.032
0.048	0.40	0.038
0.062	0.37	0.046
0.078	0.32	0.050
0.086	0.30	0.052
0.099	0.29	0.058
0.115	0.23	0.054

Table 3. Raw Data for Standpipe Pressure Drop (ΔP_{sp}) and Solids Volumetric Flux ($\overline{\nu_{sz}}$) Factorial Test

Run	Standard	ΔP_{sp} (kPa)	$\overline{\nu_{sz}}$ ($m^3\ m^{-2}\ s^{-1}$)	$-2\tau_{sw}/R$ (kN/m^3)	$-\Delta P_g/L$ (kN/m^3)	$-\Delta P_s/L$ (kN/m^3)
1	6	22.61	0.071	0.83	4.88	2.72
2	8	25.7	0.068	0.91	5.95	1.57
3	4	25.79	0.07	1.15	5.28	1.99
4	7	23.9	0.039	2	4.58	1.84
5	3	24.15	0.036	1.12	4.8	2.51
6	1	20.66	0.033	2.28	3.62	2.52
7	5	20.88	0.033	0.89	4.12	3.42
8	2	22.51	0.07	0.47	4.59	3.36

changes in the number of contacts between solid particles resulting from minute changes in solids volume fraction.

Experimentally inferred values of the stress ratio from shear stress measurements

Experimentally measured shear stress values and interpreted solids pressure measurements were used to calculate the stress ratio (μ_w/K) using a galvanized steel shear vane. This coefficient was compared to an independently measured value that was obtained from a Jenike shear cell whose internal solids contact pieces were also fabricated of galvanized steel. Abou et. al (1999) determined, theoretically, that the coefficient of friction is a function of the solids volume fraction. Jenike & Johansson Inc. directly measured the rheological properties of the coke breeze material. The angle of wall friction (δ_w), the angle of internal friction, and the bulk density all changed with normal consolidation stress, as shown in Figure 11. Using Eqs. 8 and 9 these angles were used to calculate the stress ratio (μ_w/K) as a function of bulk density, illustrated in Figure 12. These data reflected bulk densities for a static packed-bed state. The moving bed in the standpipe was operated as a packed bed for all operational values of the solids volumetric flux. Because of the significant solids pressure gradient, the solids must be assumed to be in intimate contact. Equation 7 should apply until the solids are no longer in intimate contact and the stress ratio (μ_w/K) was fully defined over this range. Unfortunately, the values of the coefficient obtained directly with the Jenike shear cell did not span the full range of operation of the packed bed. In fact, these values spanned conditions under consolidation stresses that were considerably larger than those estimated in the CFB.

Equation 11 was rewritten in terms of the shear stress; the relationship between the shear stress, weight of the bed, and gas pressure drop may be expressed as follows

$$\tau_{sw}\big|_{z=z_1} = \frac{D}{4}\left[e^{-(4\mu_w/DK)(z_2-z_1)}\right]\left(\frac{\Delta P_g}{\Delta z} + \frac{4\mu_w}{DK}P_{sz}\big|_{z=z_2} - \rho_s\varepsilon_s g\right) - \frac{D}{4}\left(\frac{\Delta P_g}{\Delta z} - \rho_s\varepsilon_s g\right) \quad (14)$$

The only unknown was the stress ratio, μ_w/K. The other variables were either directly measured or inferred as a function of volumetric flux. In Figure 13 the measured shear stress and values estimated using Eq. 14 are plotted vs. volumetric flux. Estimated values of shear stress were calculated by adjusting μ_w/K values to fit Eq. 14 to the measurements. These values are plotted with solid circles in Figure 13. At low values of the volumetric flux the coefficient dropped rapidly as the volumetric flux increased. The value of μ_w/K extrapolated back to the point of incipient flow (onset of bed movement) to the value of μ_w/K obtained directly from the Jenike shear cell, 0.059. When the Jenike shear cell value for the coefficient was used in Eq. 12 the predicted values for the shear stress resulted in the upper curve in Figure 13. In general, these predicted shear stress values were several times greater than the actual measured values. This demonstrates the inadequacy of the Jenike cell measurements for the coke breeze material in this application.

In both the steady-state and the flow ramps (Figures 9 and 10) the shear stress dropped steeply with increasing solids volumetric flux for fluxes $< 0.05\ m^3\ m^{-2}\ s^{-1}$. According to the fluctuations in the solids flow and relative velocities, the solids were in slip-stick flow regime. However, for solids volumetric fluxes > 0.055 the bed was in the smooth flow regime, where the fluctuations with respect to solids velocity were measurably smaller. The value for μ_w/K approached 0.0033 for this regime. This stress ratio was about 15 times smaller compared to that measured for stick-slip flow. However, the stress ratio changed by only about 50% once the boundary of the smooth flow regime had been exceeded ($\sim 0.05\ m^3\ m^{-2}\ s^{-1}$).

A simple power-law correlation was developed to estimate the stress ratio, μ_w/K, as a function of solids volumetric flux (Figure 14). The theory developed by Jackson (1998) and applied to CFB standpipes by Srivastava and Sundaresan (2002) indicates that μ_w/K is a constant that does not vary with increasing solids flux or volume fraction. However, measurements taken from the Jenike shear cell for this bed material, coke breeze, demonstrated that μ_w/K depended on the normal compressive force or bed density. The relationship displayed in Figure 14 bridges the gap between (1) the packed-bed friction coefficient measured in the Jenike shear cell under incipient flow conditions and (2) the coefficient observed at higher solids

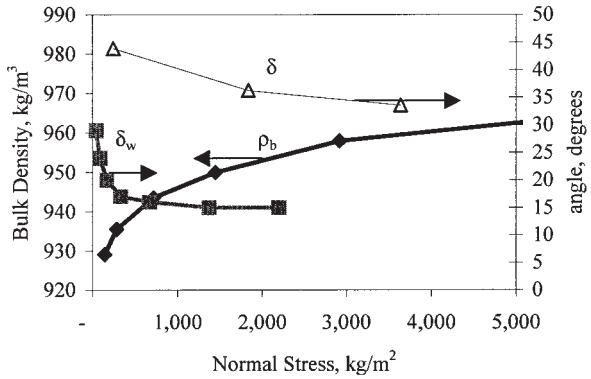

Figure 11. Rheological properties of coke breeze measured with Jenike shear cell.

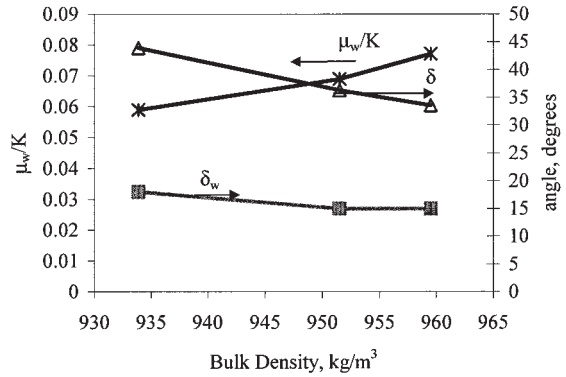

Figure 12. Variation of the stress ratio with normal stress for coke breeze.

velocities. This expression correlated the general behavior for frictional flow as the solids transition from the stick-slip regime to the smooth flowing packed regime. However, the actual value for this transition will depend on the relative gas–solids velocity, which in turn is affected by the particular features of the test rig such as the reactor geometry, configuration of the standpipe and nonmechanical valve, the standpipe bed height, and the riser flow conditions.

Equation 11 is used to generate the solids pressure profiles as a function of standpipe height shown in Figure 15. Assumptions were constant solids volume fraction, constant gas pressure drop per unit length, zero solids pressure at the top of the bed, and that the bed is in an active state of stress. Because of the assumption of constant gas pressure drop per unit length, this equation was applied over several small sections of the standpipe where measured values of the gas pressure were known and the incremental values of the solids pressure along the standpipe were determined. In the plot there is a one-to-one correspondence between solids volumetric flow rate and μ_w/K, based on the results of Figure 14. Over the reported data range the solids pressure varied linearly with height. All of the solids pressure profiles were integrated from the bed top to bottom, with the total bed height varying as a function of the solids flux.

The solids pressure drop per unit length decreased significantly as the total standpipe gas pressure drop increased (Table 3). This positively demonstrated that the packed-bed CFB standpipe was dissimilar to the open standpipe systems studied by Delaplaine (1956), in which both the gas and solids pressure drops become constant once the axial flow profile was developed. In addition, the gas pressure drop per unit length increased significantly with increasing solids volumetric flux. This reflects the behavior of a constant inventory test in which the increased standpipe aeration necessary for higher solids flow rates creates greater holdup of solids in the riser and a correspondingly higher gas pressure drop per unit length in the standpipe. The observed result was that the solids pressure drop per unit length decreased significantly as both the gas pressure drop and solids flow increased.

Conclusions

Solids-phase shear stress and pressure cannot be ignored in the momentum balance of a standpipe. Solids shear stress was experimentally measured. Using a one-dimensional, gas–solids momentum balance the solids-phase pressure was estimated. Consistent with the results of Srivastava (1998), the solid-phase pressure and solids shear stress were found to be important forces in the momentum balance. The shear stress ranged from 27 to 6% of the total force on a control volume of bed material in which the solids volumetric flux was increased from 0.01 to 0.12 $m^3\ m^{-2}\ s^{-1}$. The solids pressure drop per unit length was about 30% of the total force. This is consistent with Srivastava (1998), who found the combination of wall shear and solids pressure can be as large as 42% of the total forces. The solids pressure contribution depended on the inventory or bed height.

An attempt was made to model solids wall shear stress and solids pressure from the Jenike shear cell measurements of the bed material's flow properties independent of shear stress measurements. The values of shear stress, estimated using a stress ratio value measured from the Jenike shear cell, were up to four times the values measured in the standpipe. Further, the values of solids pressure that were estimated independently from the shear stress measurements were less than half those predicted using measured values of shear stress.

When the stress ratio was adjusted such that the predicted shear values matched the measured values, the ratio was found to vary with solids volumetric flux and it was considerably smaller than the values measured by the Jenike shear cell. This

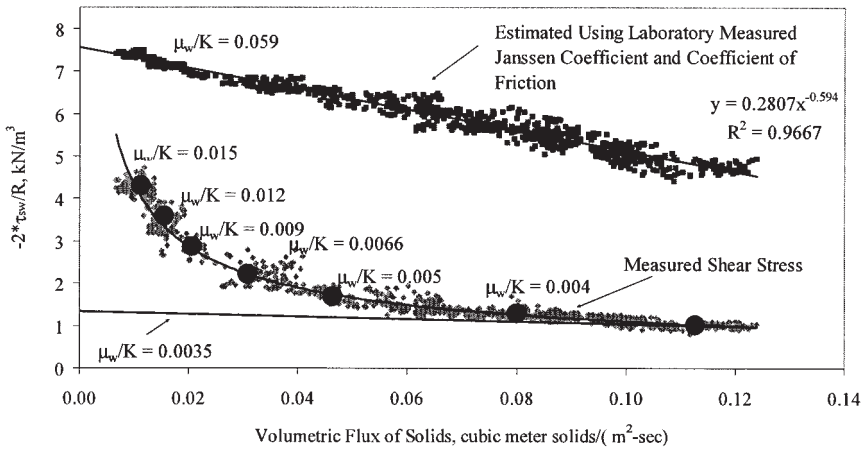

Figure 13. Measured and estimated values of $-4\tau_{sw}/D$ vs. solids volumetric flux.

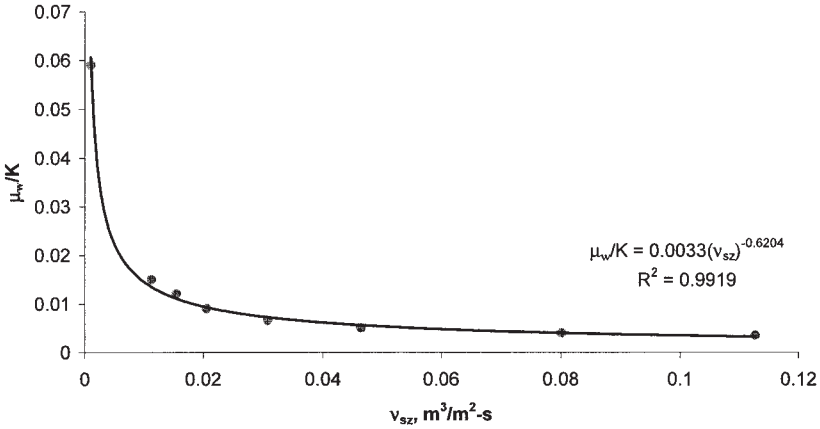

Figure 14. Fitted correlation for the stress ratio, μ_w/K, as a function of the solids volumetric flux.

suggests that the stress ratio as measured in a Jenike shear cell, under nonaerated, incipient flow conditions, was inappropriate for use in the standpipe of a CFB. In the Jenike cell the stress ratio for this bed material was found to be dependent on solids volume fraction. A correlation was developed that could be used to estimate this stress ratio for coke breeze in both the slip-stick and smooth flow regimes for packed-bed flow in the FB standpipe.

The variation of the stress ratio with solids volumetric flux was contrary to the generally accepted practice of using a constant (Hancher and Jury, 1959; Jones and Leung, 1985; Mountziaris and Jackson, 1990; Picciotti, 1995; Rangachari and Jackson, 1984). Some researchers, however, suggest that this assumption may be inaccurate (Grossman, 1975; Li and Kwauk, 1989a). Delaplaine (1956) measured radial solids pressure and solids wall shear stress and found that μ_w was independent of solids velocity, which is contrary to the findings of Brandt and Johnson (1963). The fact that Brandt and Johnson's work is with a liquid–solid system and Delaplain's work is with a gas–solid system may explain this discrepancy. Results in this study cannot validate or dispute Delaplaine's findings because only an estimate of the combination of the coefficients, μ_w and K, was determined. However, it was found that the μ_w/K combination varied with solids flux and was substantially different from the value measured using a Jenike shear cell.

Notation

A = surface area of the control volume
D = diameter of the standpipe
D_p = particle diameter
g = acceleration arising from gravity
F_z = forces acting on the control volume in the z-direction
F_m = moving air (aeration at 0.091-m height in the standpipe) aeration rate
$1/K$ = Janssen coefficient
L = control volume height
$\vec{n}$ = outward drawn normal unit vector
P_g = gas-phase pressure
P_s = solids-phase pressure
P_{sz} = solids-phase pressure in the axial direction
P_{sr} = solids-phase pressure in the radial direction
R = radius of the standpipe
SD = standard deviation
U_{mf} = superficial gas velocity at minimum fluidization
U_g = superficial gas-phase velocity
U_s = superficial solids-phase velocity
V = volume of control volume
$\vec{v}_g$ = gas-phase velocity vector
v_{gz} = gas-phase velocity in the axial direction
$\vec{v}_s$ = solids-phase velocity vector

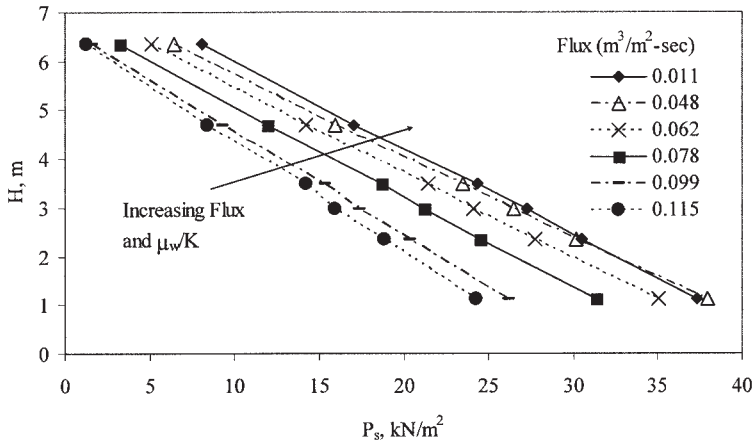

Figure 15. Solids pressure profiles as a function of solids volumetric flux.

v_{sl} = slip velocity
v_{sz} = solids-phase velocity in the axial direction, or solids volumetric flux
$\overline{v_{sz}}$ = mean solids volumetric flux in the axial direction

Greek letters

α = significance level used to estimate the confidence level ($\alpha = 0.05$ is 95% C.L.)
δ = internal angle of friction
δ_w = external angle of friction
ε = void fraction of the gas phase
ε_{mf} = void fraction of the gas phase at minimum fluidization
ε_g = void fraction of the gas phase
ε_s = volume fraction of the solids phase
$\varepsilon_{s,mf}$ = volume fraction of the solids phase at minimum fluidization
$\varepsilon_{s,v}$ = volume fraction of the solids phase under vibrating conditions
ρ_b = bulk density
ρ_g = density of gas phase
ρ_p = particle density
ρ_s = density of solids phase
σv_{sz} = standard deviation of the volumetric flux
μ_w = coefficient of friction
μ_w/K = stress ratio
τ_{sw} = solids wall shear stress
τ_{gw} = gas wall shear stress

Literature Cited

Abou-Chakra, H., and U. Tuzun, "Coefficient of Friction of Binary Granular Mixtures in Contact with a Smooth Wall. Part B. Micro-Structural Model Describing the Effects of Packing Fraction and Load Distribution on the Wall Friction of Smooth, Elastic Spheres," *Chem. Eng. Sci.*, **54**, 5913 (1999).

Bi, H., and J. Zhu, "Static Instability Analysis of Circulating Fluidized Beds and Concept of High-Density Risers," *AIChE J.*, **39**, 1272 (1993).

Brandt, H. L., and B. M. Johnson, "Forces in a Moving Bed of Particulate Solids with Interstitial Fluid Flow," *AIChE J.*, **9**, 771 (1963).

Chen, Y. M., S. Rangachari, and R. Jackson, "Theoretical and Experimental Investigation of Fluid and Particle Flow in a Vertical Standpipe," *Ind. Eng. Chem. Fundam.*, **23**, 345 (1984).

Delaplaine, J. W., "Forces Acting in Flowing Beds of Solids," *AIChE J.*, **2**, 127 (1956).

Ginestra, J. C., S. Rangachari, and R. Jackson, "A One-Dimensional Theory of Flow in a Vertical Standpipe," *Powder Technol.*, **27**, 69 (1980).

Grossman, G., "Stresses and Friction Forces in Moving Packed Beds," *AIChE J.*, **21**(4), 720 (1975).

Hancher, C. W., and S. H. Jury, "Semi-Continuous Countercurrent Apparatus for Contacting Granular Solids and Solution," *Chem. Eng. Prog. Symp. Ser. 24*, **55**, 87 (1959).

Jackson, R., "The Nature and Role of Effective Stress in Fluidized Systems," In: L. S. Fan and T. M. Knowlton, eds., *Fluidization IX*, United Engineering Foundation, New York, pp. 1–13 (1998).

Jones, P. J., and L. S. Leung, "Downflow of Solids through Pipes and Valves," In: J. E. Davidson, ed. *Fluidization*, 2nd ed. Academic Press, London (1985).

Li, H., "Mechanics of Arching in a Moving-Bed Standpipe with Interstitial Gas Flow," *Powder Technol.*, **78**, 179 (1994).

Li, H., and M. Kwauk, "Vertical Pneumatic Moving-Bed Transport—I. Analysis of Flow Dynamics," *Chem. Eng. Sci.*, **44**(2), 249 (1989a).

Li, H., and M. Kwauk, "Vertical Pneumatic Moving-Bed Transport—II. Experimental Findings," *Chem. Eng. Sci.*, **44**(2), 261 (1989b).

Ludlow, C. J., L. J. Shadle, and M. Syamlal, "Development of Spiral Device for Measuring Solids Flow." In: J. R. Grace, J. Zhu, and H. de Lasa, eds., *Circulating Fluidized Bed Technology VII*. Canadian Society of Chemical Engineering, Ottawa, Canada, pp. 513–520 (2002).

Matsen, J. M., "Flow of Fluidized Solids and Bubbles in Standpipes and Risers," *Powder Technol.*, **7**, 93 (1973).

Matsen, J. M., "Some Characteristics of Large Solids Circulation Systems," In: D. L. Keairns, ed., *Fluidization Technology*, Vol. II. Hemisphere Publishing, Washington, DC, pp. 135–149 (1976).

Mohan, L. S., P. R. Nott, and K. K. Rao, "Fully Developed Flow of Coarse Granular Materials through a Vertical Channel," *Chem. Eng. Sci.*, **52**(6), 913 (1997).

Monazam, E. R., L. J. Shadle, and L. O. Lawson, "A Method for Determining the Saturation Carrying Capacity of Gas in Circulating Fluid Beds," *Powder Technol.*, **121**, 205 (2001).

Monazam, E. R., L. J. Shadle, J. C. Ludlow, and J. Ontko, unpublished results (2004).

Mountziaris, T., and R. Jackson, "The Effects of Aeration on the Gravity Flow of Particles and Gas in Vertical Standpipes, " *Chem. Eng. Sci.*, **46**(2), 381 (1990).

Nedderman, R. M., and C. Laohakul, "The Thickness of the Shear Zone of Flowing Granular Materials, " *Powder Technol.*, **25**, 91 (1980).

Nowak, W., H. Matsuda, K. K. Win, and M. Hasatani, "Diagnosis of Multi-Solid Fluidized Beds by Power Spectrum Analysis of Pressure Fluctuations," ed., A. A. Avidan, *Circulating Fluidized Bed Technology IV*. Somerset, PA, p. 131 (1993).

Picciotti, M., "Specify Standpipes and Feeder Valves for Packed Beds, " *Chem. Eng. Prog.*, **91**(1), 54 (1995).

Rangachari, S., and R. Jackson, "The Stability of Steady States in a One-Dimensional Model of Standpipe Flow, " *Powder Technol.*, **31**, 185 (1982).

Sarra, A. M., *Particle-Wall Shear Stress Measurements within the Standpipe of a Circulating Fluidized Bed*, MS Thesis, West Virginia University, Morgantown, WV (2001).

Shadle, L. J., J. C. Ludlow, L. O. Lawson, and E. R. Monazam, "Transport Reactor Studies in FETC's Cold Flow Circulating Fluid Bed," Transport Reactor Cooperative Research and Development Agreement Report, CRADA No. 98-F015, U.S. Dept. of Energy, National Energy Technical Laboratory, Morgantown, WV (1999).

Srivastava, A., K. Agrawal, S. Sundaresan, S. B. R. Karri, and T. M. Knowlton, "Dynamics of Gas-Particle Flow in Circulating Fluidized Bed," *Powder Technol.*, **100**, 173 (1998).

Srivastava, A., and S. Sundaresan, "Role of Wall Friction in Fluidization and Standpipe Flow," *Powder Technol.*, **124**, 45 (2002).

Takahshi, H., and H. Yanai, "Flow Profile and Void Fraction of Granular Solids in a Moving Bed," *Powder Technol.*, **7**, 205 (1973).

Tuzun, U., and R. M. Nedderman, "Experimental Evidence Supporting Kinematic Modeling of the Flow of Granular Media in the Absence of Air Drag," *Powder Technol.*, **24**, 257 (1979).

Zhang, J., P. Jiang, and L. S. Fan, "Dynamic Behavior in Transients of Solids Flow Rates in a Circulating Fluidized Bed System," In: L. S. Fan and T. M. Knowlton, eds., *Fluidization IX*. United Engineering Foundation, New York (1998).

Zhang, J., and V. Rudolph, "Flow Instability in Non-Fluidized Standpipe Flow," *Powder Technol.*, **97**, 109 (1998).

Manuscript received Jan. 31, 2003, and revision received July 22, 2004.